Faulty Phase Identification Using Probability Tail Function for EHV Transmission Systems

N. I. Elkalashy, M. Lehtonen

Abstract--**In this paper, a novel simplified probabilistic technique is investigated to identify the faulty phase. Estimating the faulty phase enhances the operation of single-pole autoreclosure which is applied in Europe countries. The proposed technique is based on the probability tail functions applied on the standard deviations of Discrete Wavelet Transforms (DWT) of the phase currents. An adaptive setting is proposed to be suitable for different faulty phase. The setting signal is selected as the maximum standard deviation of the DWT of phase currents. The earth faults and phase faults are correctly discriminated. Validation of the proposed algorithm is verified via ATP/EMTP simulation. Test results corroborate evidence of the efficacy of proposed technique.**

I. Introduction

A concept of single pole autoreclosure has been adopted by several electricity authorities in Europe in order to improve the system dynamic stability. A closing decision is usually issued post-faulted phase isolation considering a suitable delay time. Therefore, discriminations of faulty phase from the healthy ones are highly recommended to avoid tripping of the incorrect phase or unnecessary three-phase tripping, thereby minimizing system insecurity and instability [1]-[2].

Recently, high frequency transients generated due to fault occurrence have been used to estimate the faulty phase as reported in [2]-[3]. The Neural Network was trained to different fault types in [2]-[3]. However, the neural network can not efficiently work when it is exposed to some patterns outside the training classes; therefore, the neural network relays are not portable to different power networks. In [2], the traveling waves of measured voltage signals have been extracted using Fast Fourier Transform (FFT). The shortcoming of FFT can be overcome using Wavelet Transform as considered in [3] where the transients incorporated in the current waveforms are extracted using Discrete Wavelet Transform (DWT).

Probability techniques have been recently used to enhance the fault detection in distribution networks as reported in [4]-[5]. However, such techniques have been used to identify the faulty feeder in high impedance earthing distribution networks.

N. I. Elkalashy and M. Lehtonen are with Power Systems and High Voltage Engineering, Department of Electrical Engineering, Faculty of Electronics, Communications and Automation, Helsinki University of Technology (TKK), Finland (e-mail: nagy.elkalashy@tkk.fi; Fax:+35894515012).

Paper submitted to the International Conference on Power Systems Transients (IPST2009) in Kyoto, Japan June 3-6, 2009

In this paper, the faulty phase is identified using a simplified probabilistic method applied on the DWT-based extracting transient features. The algorithm performance is verified for resistive fault and arcing fault types. The algorithm procedure is depending on standard deviations of DWT detail coefficients of the phase currents. A novel discriminator is investigated to estimate the faulty phase where it is depending on the probability that the phase random transient currents will exceed a given threshold. This probability is found suitable for discriminating between the healthy and faulty phases. A practical 400 kV transmission line is simulated in ATP/EMTP where ATPDraw is used as a graphical interface. The fault model is incorporated at different locations and the considered arcs are implemented using a universal arc representation.

II. Proposed Algorithm

The proposed technique mainly depends on DWT and probability for the fault detection. The detection process is divided into feature extraction using DWT and then the decision using a probabilistic method. A small introduction on DWT is in Appendix A. The probability concept and the detection technique are discussed in following paragraphs.

Faults introduce transients to the otherwise clean sinusoidal current and voltage waveforms of the power system. These transients are small and random fluctuations that last for a short period of time. When the phase currents are analyzed using the DWT, the details signal will exhibit the randomness generated by the fault. Since the details signal is composed of the sum of several random components, the derails signal can be approximated by the Gaussian distribution according to the central limit theorem. This can be confirmed by applying the Kolmogorov-Smirnov normality test. Hence, the probability density function (pdf) of the *i*-th phase current details signal d_i is given by:

$$f_{d_i}(x) = \frac{1}{\sqrt{2\pi}\sigma_i} \exp\left[-\frac{x^2}{2\sigma_i^2}\right] \quad (1)$$

where σ_i is the standard deviation of the details of the *i*-th phase. Then the probability that this random signal is greater than threshold *A* can be written as:

$$P_i = \Pr\{d_i > A\} = \frac{1}{\sqrt{2\pi}\sigma_i} \int_A^\infty \exp\left[-\frac{x^2}{2\sigma_i^2}\right] dx \quad (2)$$

This is the well-known probability tail function where it is equal to one minus the cumulative distribution function of the

standardized normal random variable. It can be written in terms of the Q-function as [5]-[6]:

$$P_i = \mathrm{Q}\left(\frac{A}{\sigma_i}\right) \tag{3}$$

where the Q-function is defined as:

$$\mathrm{Q}(k) = \frac{1}{\sqrt{2\pi}} \int_k^{\infty} \exp\left[-\frac{x^2}{2}\right] dx \tag{4}$$

The scenario of the fault detection and its location can be understood with the aid of Fig. 1. At each measuring node, phase currents are measured and they are analyzed using DWT to extract the transients generated due to fault occurrences. The standard deviation (*Sdt*) is computed over a power cycle sliding window of the DWT detail level d1. The selectivity function to estimate the faulty phase is proposed based on the Q-function as in (3) where the threshold value *A* is maximum standard deviation of the DWT detail d1 of phase currents. To improve the algorithm stability during normal operation to avoid the noises as well, the minimum threshold value is considered equal to 0.1, which means that if the maximum standard deviation of the DWT detail d1 of phase currents is less than 0.1, the *A* is fixed at 0.1. Due to fault occurrence, the expected value of Q-function of the faulty phase is Q(1) which is the highest one. Therefore, the Q-function of each phase is divided by Q(1) to get a discriminator *P* equal to one however the discriminator of the other phases are less.

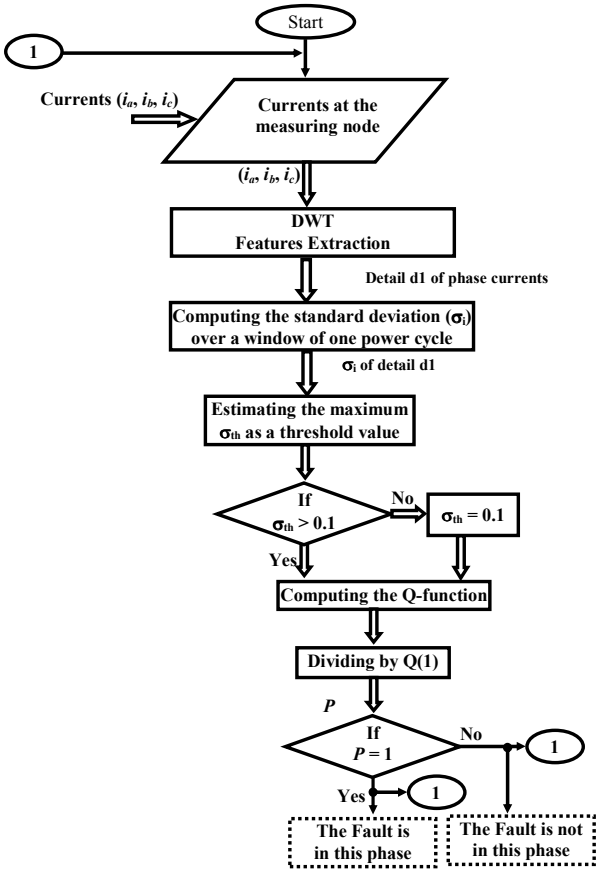

Fig. 1 Implementation of the proposed detection technique.

As aforementioned, the proposed algorithm depends on DWT and probability. Regarding the DWT, several wavelet families are tested to extract the fault features using the Wavelet toolbox incorporated into the MATLAB program [7]. Daubechies wavelet 14 (db14) is appropriate for fault transient localization. The Details d1 including the frequency band 3.2-6.4 kHz are investigated, in which the sampling frequency is 12.8 kHz. Increasing the sampling frequency improves the proposed technique performance where the best performance is attained when the travelling waves due to fault event are fully extracted.

III. Performance Evaluation

A. Simulated Transmission Power System

Figure 2 illustrates the single line diagram of a 400 kV transmission line simulated in the ATP/EMTP program. The ATPDraw program is used as preprocessor [8]. The line length is 144 km and it is represented using a frequency dependent JMarti model as discussed in Appendix B.

One of the most verified models for representing the arcing faults is the thermal model of Kizilcay, in which, a synthetic test circuit is developed to obtain the parameters of primary and secondary phases of the arc along a 380-kV insulation string [9]. The arcing fault equation of this model is written as:

$$g = \int \frac{1}{\tau}(G - g)dt \tag{5}$$

$$G = \frac{|i|}{u_{st}} \tag{6}$$

$$u_{st} = (u_o + r|i|)l \tag{7}$$

where g is time-varying arc conductance, G is stationary arc conductance, τ is arc time constant, r is the resistive component per arc length, u_o is constant voltage per arc length, l is time dependent arc length, and i is arc current. Primary arc parameters are: l is 350cm, τ is 1.3ms, u_o is 12 V/cm, and r is 1.3 mΩ/cm [9].

Considering the bilateral interaction between the EMTP network and TACS filed, the arcing fault equations are implemented using the universal arc representation [10] as described in Fig. 3. The arc current is transposed into TACS field using sensors types 91. The arc equations (5), (6), and (7) are solved in the TACS exploiting integrator device type 58 with the aid of FORTRAN expressions. Thereafter, the computed arc resistance is sent back into the network in the next step and so on. Accordingly, the arcing fault interaction is performed. The aforementioned power system and the fault element are combined in a single arrangement to investigate the performance of proposed technique.

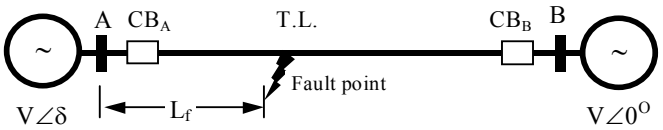

Fig. 2. Simulated transmission system.

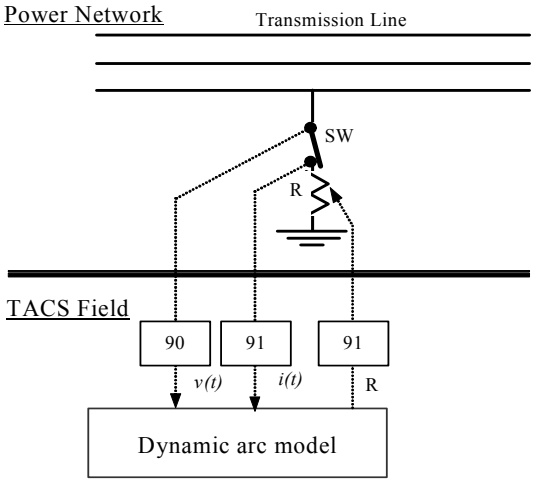

Fig. 3 EMTP network of arcing fault interaction.

B. Earth Faults

In this subsection, the proposed algorithm in section 2 is evaluated during earth faults. Fig. 4 illustrates phase currents measured at both ends of the transmission line during phase-a to ground fault occurred at 50 km from Bus A. The fault instant is at 32 ms. The corresponding DWT details level d1 is shown in Fig. 5 where the transients generated due to fault occurrence are extracted at Bus A and B. It is obvious that the transient features are found in all phases; however, they are small in magnitude. Also, it is expected a delay due to DWT usage; however, such delay is depending on the DWT filter samples. This delay will be some samples and it is a fraction of *ms*. Also, these transient are generated at the fault instant during a quarter-cycle and they can provide fast response for faulty phase identification. Therefore, the standard deviation (*Sdt*), which is computed over a power cycle sliding window of the DWT detail level d1, can be alternatively computed over quarter-cycle sliding window.

Accordingly, the performance of the proposed algorithm is shown in Figs. 6 and 7. Fig. 6 illustrates the standard deviation measured where the transients are localized in the three phases; however, the standard deviation of the faulty phase is the highest one. Accordingly, Fig. 7 illustrates the faulty phase discriminator performance where the discriminator of phase-a is one; however, the discriminator of other phases are under one. Such performance correctly indicate to the faulty phase-a.

To improve the security of proposed technique, the discriminator output is accepted when the discriminator values of healthy phases are equal which means the DWT detail d1 of these phases are equal. In that way, the security is enhanced to overcome the shortcoming during two phases to ground fault type as it is discussed in the following subsection. The validity of this security is examined considering different fault instants such as fault occurrences at 24, 26, 28, and 30 ms and at different fault locations such as 20, 50, 75 and 125 km. Table 1 summarizes the standard deviation (*Std*) values of the DWT detail d1 measured at Bus A and Bus B using these fault conditions. The highest *Std* is of the faulty phase and the *Std* values of other phases, which are healthy, are equal.

Table 1: The Discriminator P for healthy phases.

Fault Instant, Location	Discriminator at Bus A		Discriminator at Bus B	
	$P_{IA\,b}$	$P_{IA\,c}$	$P_{IB\,b}$	$P_{IB\,c}$
24 ms, 50 km	0.4578	0.4580	0.2279	0.228
26 ms, 50 km	0.1737	0.1737	0.2572	2572
28 ms, 50 km	0.1742	0.1742	0.3652	0.3652
30 ms, 50 km	0.5975	0.5975	0.6161	0.6161
32 ms, 50 km	0.2009	0.2009	0.4720	0.4720
32 ms, 20 km	0.1213	0.1213	0.1915	0.1915
32 ms, 75 km	0.2379	0.2379	0.2861	0.2861
32 ms, 125 km	0.2516	0.2516	0.0374	0.0374

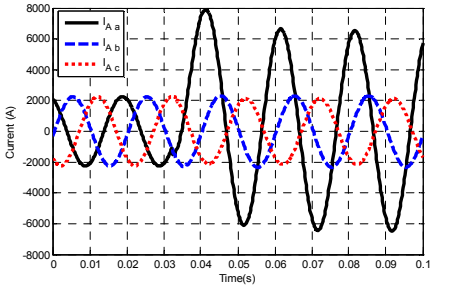

a. Currents measured at Bus A

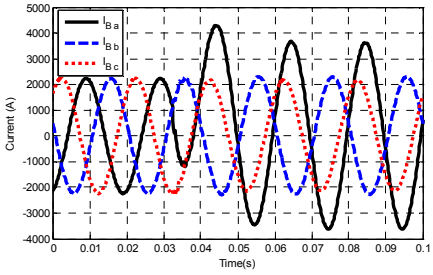

b. Currents measured at Bus B

Fig. 4. Simulated waveforms for Phase-a to ground fault at 50 km.

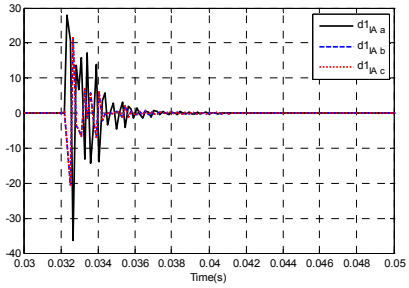

a. At Bus A.

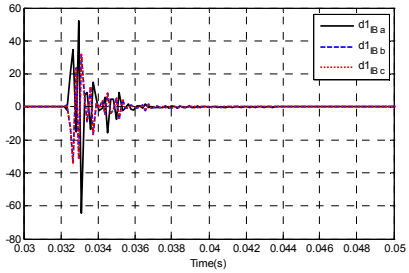

b. At Bus B.

Fig. 5. DWT detail level d1 for fault case shown in Fig. 3.

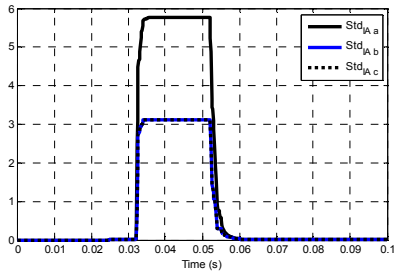

a. At Bus A.

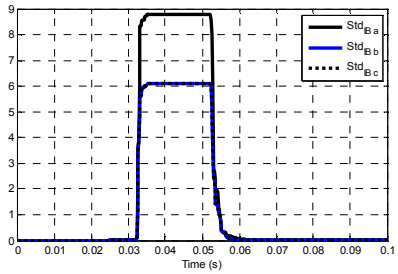

b. At Bus B.

Fig. 6. The standard deviation of DWT detail d1 shown in Fig. 5.

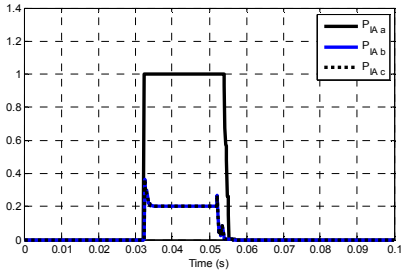

a. At Bus A.

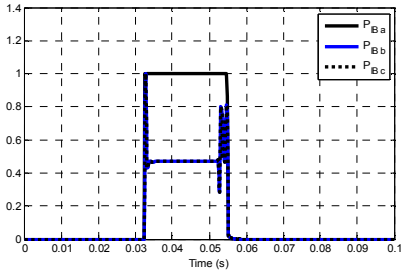

b. At Bus B.

Fig. 7. The discriminator performance during the earth fault case.

Fig. 8 illustrates the proposed algorithm for arcing fault case occurred at 40 km. The faulty phase is correctly identified. As the discriminator of Phase-b and Phase-c have the same values during the discriminator of Phase-a is one, the security function is achieved as well.

C. Phase Faults

Fig. 9 illustrates the DWT detail d1 and the discriminator performance during phase fault case occurred at 32 ms and its location is at 50 km where the fault is between phases a and b. In Figs. 9.a and b, the initial transients are only localized in faulty phases a and b at both ends of the line. The corresponding performance of the discriminator at Bus A and B is shown in Figs. 9. c and d, respectively where the proposed technique can estimate the fault type is phase fault type as two discriminators are one while the third one is zero.

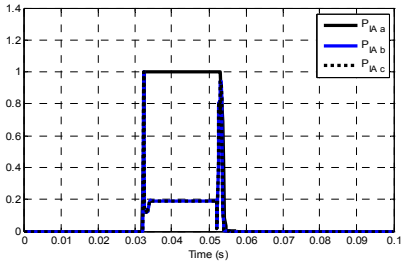

a. At Bus A.

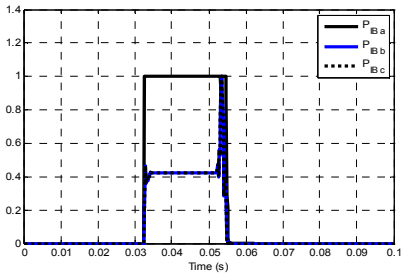

b. At Bus B.

Fig. 8. The performance during the arcing fault case at 40 km.

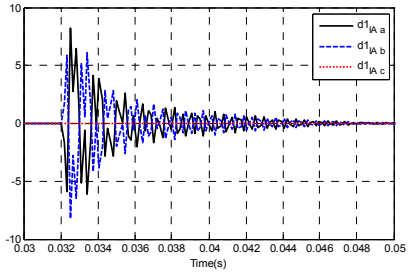

a. DWT detail level d1 at Bus A.

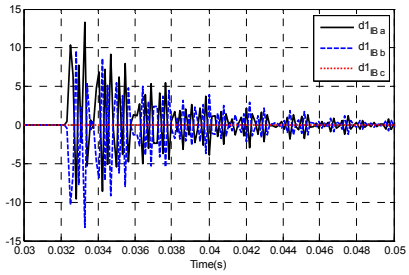

b. DWT detail level d1 at Bus B.

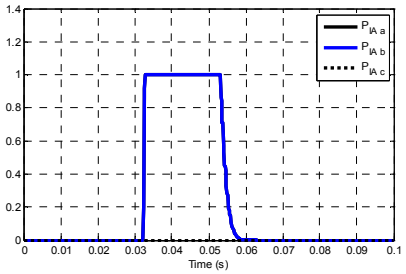

c. Discriminator performance at Bus A.

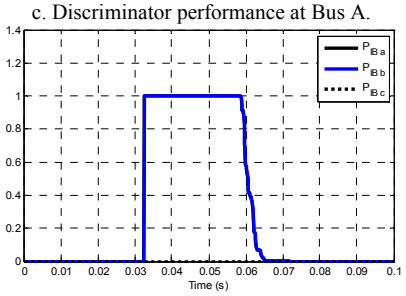

d. Discriminator performance at Bus B.

Fig. 9. The performance during the phase fault case at 50 km.

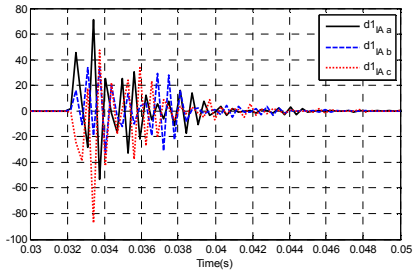

a. DWT detail level d1 at Bus A.

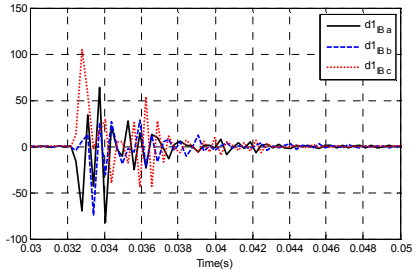

b. DWT detail level d1 at Bus B.

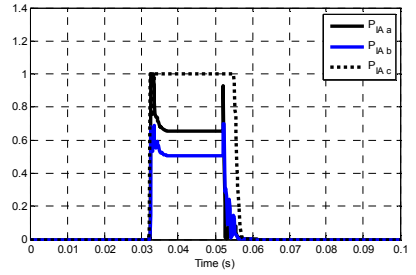

c. Discriminator performance at Bus A.

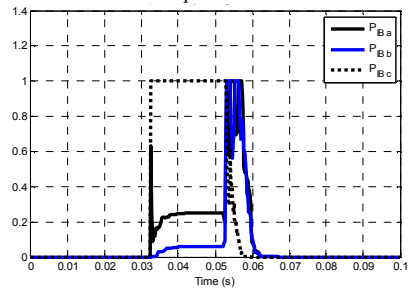

d. Discriminator performance at Bus B.

Fig. 10. The performance during the phase a-b to ground fault case.

On the other hand, when the fault is phase a to b to ground fault, the corresponding performance is shown in Fig. 10. The transients are localized in all phases at both Bus A and B as depicted in Fig. 10.a and b, respectively. In Figs. 10.c and d, the performance is indicating that the faulty phase is phase c, however, the discriminator of other phases are not equal. Therefore, the fault is not phase to ground fault as the security condition is not achieved.

For a three-phase fault case occurred at 32 ms and its location is at 50 km, Fig. 11 illustrates the discriminator performance where the lowest Discriminators, which are phase a and b, are not equal. Therefore, the fault is phase type not earth fault type.

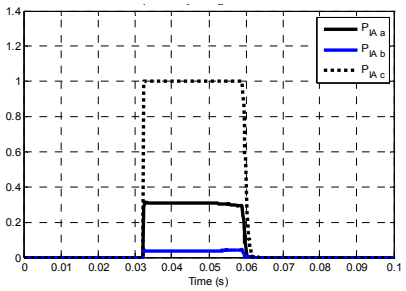

a. At Bus A.

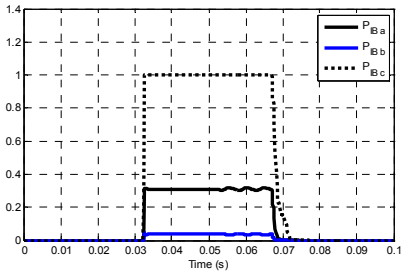

b. At Bus B.

Fig. 11. The performance during three-phase fault at 50 km.

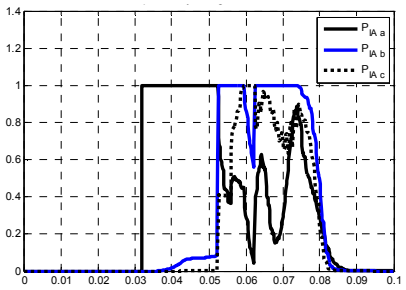

a. At Bus A.

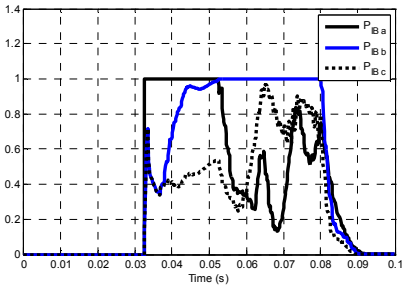

b. At Bus B.

Fig. 12. The performance during switching of Bus A.

D. Switching

Fig. 12 illustrates the performance during switching case when the switch at Bus A is closed at 32, 36 and 42 ms for phases-a, b and c, respectively. The transients are localized in all phases, however, the probability of the lowest two phases are not equal. Therefore, these transients are not due to earth faults and the discriminator response could not be taken into account. For another switching case where the closing of breaker poles are simultaneous at 32 ms, the security is also attained; however, this test case is not presented as the breaker poles are not practically closing simultaneously.

IV. Conclusions

Performance of a simplified probabilistic approach for identifying phase faults has been investigated. The fault features have been extracted using DWT. The standard deviation of the DWT phase currents has been computed to localize the fault transients. The technique performance has been evaluated considering different fault types; earth and phase faults and considering switching as well. Therefore, sensitive and secure detection of the faulty phase has been attained using DWT and probability.

V. Appendix

A. DWT

Wavelets are families of functions generated from one single function, called the mother wavelet, by means of scaling and translating operations. The scaling operation is used to dilate and compress the mother wavelet to obtain the respective high and low frequency information of the function to be analyzed. Then the translation is used to obtain the time information. In this way, a family of scaled and translated wavelets is created and it serves as the base for representing the function to be analyzed [11]. The DWT is in the form:

$$DWT_{\psi} f(m,k) = \frac{1}{\sqrt{a_o^m}} \sum_n x(n)\psi\left(\frac{k - nb_o a_o^m}{a_o^m}\right) \quad (6)$$

where $\psi(.)$ is the mother wavelet that is discretely dilated and translated by a_o^m and $nb_o a_o^m$, respectively. a_o and b_o are fixed values with $a_o>1$ and $b_o>0$. m and n are integers. In the case of the dyadic transform, which can be viewed as a special kind of DWT spectral analyzer, $a_o=2$ and $b_o=1$. DWT can be implemented using a multi-stage filter with down sampling of the output of the low-pass filter.

B. Simulated System

Fig. 13.a illustrates the considered ATPDraw network. It contains the transmission system shown in Fig. 2 and the universal arc representation illustrated in Fig. 3. The transmission line is represented using a frequency dependent JMarti model where the configuration is shown in Fig. 13.b. Thevenin's equivalent impedances at busses A and B are described using mutual coupled R-L circuit as: the positive sequence is R1= 1.0185892 Ω and L1= 50.9295 mH, and the zero sequence is R0= 2.0371785 Ω and L0= 101.85891 mH.

VI. References

[1] N. Elkalashy, H. Darwish, A-M. Taalab, and M. Izzularab, "An Adaptive Single Pole Autoreclosure Based on Zero Sequence Power" *Electric Power Systems Research*, vol. 77, no. 5-6, pp. 438-446, April 2007.

[2] Z. Bo, R. Aggarwal, A. Johns, H. Li and Y. Song "A new Approach to Phase Selection Using Fault Generated High Frequency Noise and Neural Networks" IEEE Transactions on Power Delivery, Vol. 12, No. 1, pp. 106-115, Jan. 1997.

[3] P. Silveira, R. Seara and H. Zurn "An Approach Using Wavelet Transform for Fault Type Identification in Digital Relaying" IEEE Power Engineering Society Summer Meeting, Edmonton, Alta., Canada, 18-22 July 1999.

[4] S. Hanninen, M Lehtonen and U. Pulkkinen "A Probabilistic Method for Detection and Location of Very High Resistive Earth Faults" *Electric Power System Research*, vol. 54, no. 3, pp. 199-206, June 2000.

[5] N. Elkalashy, N. Tarhuni and M. Lehtonen "Simplified Probabilistic Selectivity Technique for Earth Fault Detection in Unearthed MV Networks" Accepted at IET Transactions on Generation, Transmission and Distribution.

[6] Handbook of Mathematical Functions: With Formulas, Graphs, and Mathematical Tables, edited by Milton Abramowitz and Irene A. Stegun, Tenth edition, 1972.

[7] *Wavelet Toolbox for MATLAB*, Math Works 2005.

[8] L. Prikler and H. Hoildalen, *ATPDraw users' manual*, SINTEF TR A4790, Nov. 1998.

[9] M. Kizilcay and T. Pniok, "Digital Simulation of Fault Arcs in Power systems," *Europe Transaction on Electrical Power System, ETEP*, vol. 4, no. 3, pp. 55-59, Jan./Feb. 1991.

[10] H. Darwish and N. Elkalashy "Universal Arc Representation Using EMTP," *IEEE Trans. on Power Delivery*, Vol. 2, no. 2, pp 774-779, April 2005.

[11] M. Solanki, Y. Song, S. Potts and A. Perks "Transient protection of transmission line using wavelet transform" Seventh International Conference on Developments in Power System Protection,(IEE), pp. 299–302, 9-12 April 2001.

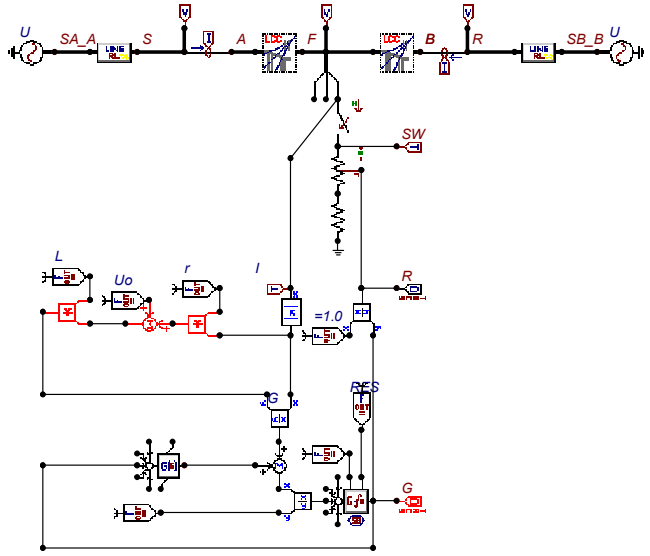

a. ATPDraw network

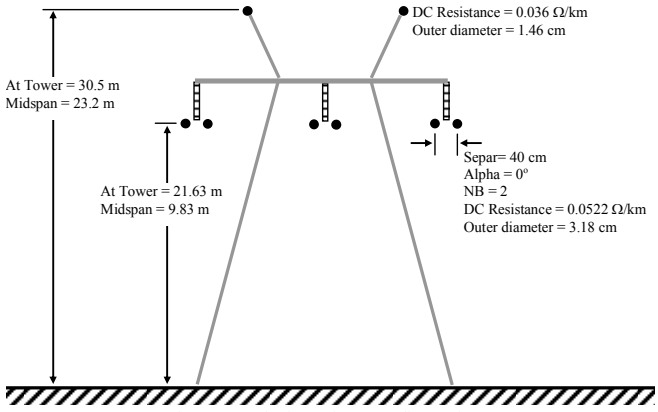

b. Transmission Line Configuration

Fig. 13 Simulated Systems.